Prediction of steady-state two-phase flow of nitrogen + extinguishant in the pipeline and a correlation for mass flow rate

Siyuan Liu[a], Yongqi Xie[a,*], Mendong Chen[b], Joanna Rawska[c], Hongwei Wu[c,**], Jianzu Yu[a]

[a]School of Aeronautic Science and Engineering, Beihang University, Beijing, 100191, China

[b]Global Energy Interconnection Research Institute, Beijing, 102200, China

[c]School of Physics, Engineering and Computer Science, University of Hertfordshire, Hatfield, AL10 9AB, United Kingdom

[*]Corresponding author: Tel: +86(10) 8233 8952, E-mail: xyq@buaa.edu.cn

[**]Corresponding author: Tel.: +86(10) 8231 7528, E-mail: h.wu6@herts.ac.uk

Acknowledgement

The authors would like to acknowledge the financial support from University of Hertfordshire, United Kingdom. This work was supported by China helicopter design and research Institute.

Prediction of steady-state two-phase flow of nitrogen + extinguishant in the pipeline and a correlation for mass flow rate

Abstract

Nitrogen used for pressurization of a fire extinguisher could be partially dissolved in the fire extinguishing agent, forming a binary mixture accompanied by a phase change while flowing inside the pipeline. Notwithstanding the widespread use of fire extinguishing system, an effective method has never been considered to predict two-phase flow performance of nitrogen + extinguishant in the pipeline. This paper presents investigation of the steady-state two-phase flow of extinguishant in the pipeline, including C_3HF_7 (HFC227ea), CF_3I, and C_2HF_5 (HFC125). The average viscosity of mixture was calculated using six quoted methods (VM-1 to VM-6). Subsequently, inspired by one-dimensional adiabatic isenthalpic flow of refrigerant in a capillary tube, the corresponding prediction models (STFM-1 to STFM-6) for large mass flux nitrogen + extinguishant in a fire extinguishing pipeline were developed based on the VM-1 to VM-6. In comparison with previous experimental and theoretical data, the applicability and accuracy of the proposed mathematical models was examined from two different aspects, mass flow rate and pressure drop. The results indicated that both models, STFM-2 and STFM-3, predicted accurately for mass flow rate, and STFM-2 model predicted accurately for pressure drop. Finally, new correlations for mass flow rate and pressure drop have been established accurately based on summarizing the relevant predicted data, respectively. This work contributes to a good theoretical approach on the analysis of two-phase flow of nitrogen + extinguishant.

Keywords: steady-state two-phase flow; adiabatic isenthalpic expansion; average viscosity; mass flow rate; pressure drop

Nomenclature

T'	presumptive temperature
r'	parameter of the PRμ model defined in Eq. (5)
p	pressure, Pa
μ	dynamic viscosity, 10^{-7} Pa·s

a	cohesive energy parameter of the PR EOS; parameter of the PRμ model, Pa m^6 mol^{-2}
b	volumetric parameter of the PR EOS; parameter of the PRμ model, m^3 mol^{-1}
T_d	a specific temperature for correction of the calculated viscosities in Eq. (2), K
r_c	parameter of the PRμ model in Eq. (8)
M_w	molar mass, g·mol^{-1}
Z_c	critical compressibility factor
c_0, c	correction terms of viscosity defined in Eq. (9)
ρ	density, kg·m^{-3}
x	gas quality
G	mass velocity, kg m^{-2}·s^{-1}
u	velocity of gas-liquid two-phase flow, m·s^{-1}
h	specific enthalpy, J·kg^{-1}
f	friction factor
d	inner diameter of pipeline, m
L	length of the pipeline, m
Re	Reynolds number
h	specific enthalpy, kJ·kg^{-1}
h_0	stagnation enthalpy, kJ·kg^{-1}
$\dot{m}$	mass flow rate, kg·s^{-1}
m	mass, kg
z	coordinate along the pipe wall in the fluid mainstream direction
V_b	volume of fire extinguishing bottle, m^3
Greek letters	
β	pressure dependent function
Superscripts	
VTPR	calculated by VTPR model
PR	calculated by PRμ model
N	nitrogen

E fire extinguishing agent

Subscripts

r reduced property

v, l gas or vapor phase, liquid phase

vo, lo gas or vapour phase with total flow, liquid phase with total flow

c critical point

m mixture

i, *j* component identification

tp two-phase mixture

b fire extinguishing bottle

p pipeline

max, min maximum, minimum

0 initial state

1, 2 inlet, outlet

f, a, g friction, acceleration, gravity

1 Introduction

A fire extinguishing system is an important aspect of fire safety design of a helicopter. In the 1990s, Halon 1301 was widely used as the fire extinguishing agent; however, green halon alternatives are being produced and used for protecting the environment in recent years [1], such as HFC227ea, CF_3I, FC218 and HFC125. In order to release the extinguishant rapidly and put out the fire efficiently, fire extinguishing bottle is usually pre-filled with nitrogen, which provides the driving force during release [2]. As the extinguishing agent is released, the nitrogen in the bottle may escape and cause the extinguishant to change from a single phase to gas-liquid phase. Due to the existence of frictional and local resistance, the temperature and pressure of nitrogen + extinguishant vary rapidly along the pipeline before the mixture reaches a new equilibrium phase.

In halogenated hydrocarbon fire-extinguishing systems, the spraying time of extinguishant is required to be very short. Therefore, as the two-phase nitrogen + extinguishant flows in the pipeline, the heat transferred to the two-phase flow through the pipe wall is principally ignored and thus regarded as adiabatic flow. Two typical filling pressures of 2.5 MPa and 4.2 MPa are always applied [2]. After the extinguisher valve is opened, the pressurised nitrogen and fire extinguishing agent vapor drive the liquid extinguishant to promptly fill the fire extinguishing pipeline, which leads to the "front end" (the part in contact with the outside) of the liquid extinguishant reaching the critical two-phase state [3, 4]. Due to the high saturated vapor pressure, it is common for liquid fire extinguishing agent to change phase as its pressure gradually decreases along the pipeline, thus becoming the main source of gas in the pipeline. Consequently, it is of great significance to study the two-phase flow for nitrogen + extinguishant to accurately calculate two-phase flow pressure drop.

The pressure drop in the two-phase flow is directly affected by viscosity. The calculation of viscosity based on $p\mu T$ equation is suitable for both gas and liquid components, with a good thermodynamic consistency. For example, Wang et al. [5] proposed a unified viscosity and density calculation model for hydrocarbon fluid by modifying the Peng-Robinson (PR) EOS; Fan et al. [6] introduced volume translation method to improve the prediction accuracy of liquid viscosity, and summarised it into volume-translated Peng-Robinson viscosity (VTPRμ) equation.

During the last few decades, some scholars have carried out experimental research on the two-phase flow of fire extinguishing agent in pipeline. Pitts and Yang et al. [3, 4] carried out the experimental research on the gas-liquid two-phase flow of four types of agents (Halon 1301, HFC125, HFC227ea, CF_3I) dissolved nitrogen with six types of pipeline layout, and , and obtained a large amount of credible two-phase flowing data. Kemal et al. [7] built a one-dimensional flow experiment platform for fire extinguishing agent, including HFC227ea, HFC125, water, and CO_2, and finally developed a one-dimensional flow calculation module (FSP) for fire extinguishing agent by using RELAP5 software. In addition, Vacek and Vins [8] measured mass data of adiabatic throttling experiments on pure FC218 and N_2 + FC218 in horizontal pipes, based on which, a two-phase critical mass flow rate prediction model was established including the unstable region of superheated liquid and two-phase flow. Moreover, Vacek et al. [9] carried out more in-depth adiabatic throttling experiments on the FC218 dissolved nitrogen, and found that the existence of nitrogen made the starting position of the two-phase flow significantly earlier than that of pure FC218, leading to the decrease of the mass flow rate through the capillary.

What's more, the two-phase flow of refrigerant in a capillary tube has been studied extensively [10-16]. The throttling process of the refrigerant in a capillary tube is commonly approximated to adiabatic isenthalpic expansion [15, 16], which is very similar to that of the fire extinguishing agent filling up a pipeline. It must be noted that the homogeneous flow model was selected in most of the studies listed above, which have shown that the refrigerant and its mixture in a capillary tube could reach critical flow state predominantly at the end of a horizontal or spiral tube due to pressure loss [17]. The critical mass flow rate was affected by multiple factors such as tube length, inner diameter, fluid sub-cooling degree, condensation pressure and refrigerant type [13, 14]. Furthermore, compared with the mass flow rate in the release process of extinguishing agent, that of all working fluids in the open literature is one or more order of magnitude smaller. Therefore, it is essential to complete more calculations and conduct further analysis of the above models to validate if they are suitable for large mass flux two-phase flow of nitrogen + extinguishant mixture in a pipeline.

In terms of pressure drop of a two-phase flow in pipelines, many researchers have presented two-phase pressure drop prediction models based on considerable amount of experimental data of refrigerants [18-24]. However, various prediction models have different accuracy for specific fluid media, and actually there is not a general model well suited for all two-phase pressure drop calculations, especially for that of extinguishant at so high pressure.

To the best of authors' knowledge, there are few detailed theoretical studies available regarding the two-phase flow of nitrogen + extinguishant in a pipeline, making the development of two-phase flow of the fire extinguishing system more unfavourable. Therefore, the aim of the current work is to propose an effective method to predicting the two-phase flow performance of the binary mixture of nitrogen + extinguishant in a pipeline. The fire extinguishing agents comprise HFC227ea, CF_3I, and HFC125. Combining with VTPRμ EOS and improved mixing rule, the methods for two-phase mixture viscosity are offered based on the six collected average viscosity formulae. Moreover, assumed one-dimensional adiabatic isenthalpic expansion process, the six corresponding models for steady-state two-phase flow of nitrogen + extinguishant are established. Additionally, the solution of the models is implemented by the finite volume method. Compared with previous experimental and calculated data, the mass flow rate and pressure drop based on different models are calculated and their accuracy is analysed. Furthermore, the mass flow rate and pressure drop in the pipeline are correlated, respectively, so that it can be applied to predict the two-phase flow performance of nitrogen + extinguishant conveniently.

2 Theory

2.1 Average viscosity

Fig. 1 presents the diagram of nitrogen-extinguishant binary mixture release process in the pipeline. At the stable state, the upper part of the fire extinguishing bottle contains nitrogen and agent vapor, while agent and dissolved nitrogen is in the lower part. After opening the valve, the two-phase flow will enter the pipeline assuming that the initial pressure is constant. The existing experiments show that the mixture of nitrogen and fire extinguishing agent may occur phase change flowing along the fire-extinguishing pipeline [3, 4].

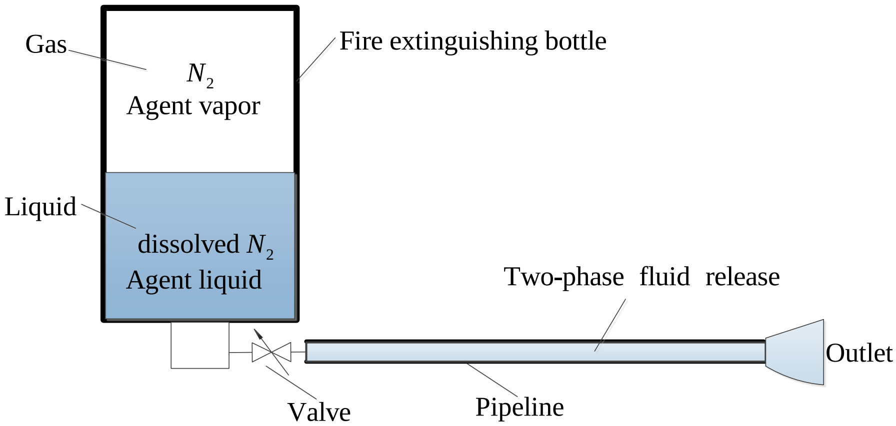

Fig. 1 The schematic diagram of release process

Viscosity as a significant physical property is frequently used in the calculation of two-phase flow in a pipeline, especially frictional pressure drop. Therefore, a prediction method suitable for viscosity of gas-liquid two-phase mixture must be proposed. As the initial filling pressure p_0 and temperature T_0 of the two-phase equilibrium system are given, the thermodynamic state of nitrogen and fire extinguishing agent can be ascertained based on the Gibbs phase rule [25-27]. Then, the thermodynamic path of adiabatic isenthalpic expansion can also be obtained, where the appropriate EOS and mixing rule must be specified.

In terms of the former, the Peng-Robinson (PR) EOS [28] is one of the most common equations during engineering phase equilibrium calculation. Due to the similarity between pvT and $p\mu T$

relationships, Fan and Wang [6] proposed the corresponding viscosity model named PRμ model based on PR EOS, which can be written as:

$$T' = \frac{r'p}{\mu - b} - \frac{a}{\mu^2 + 2b\mu - b^2} \tag{1}$$

where: μ is the dynamic viscosity, 10^{-7} Pa·s; T' denotes the presumptive temperature calculated based on the following:

$$T' = T - T_d\,,\;\; T_d = 0.45T_{\mathrm{c}} \tag{2}$$

The subscript c refers to critical state.

With the definition of Eq. (1):

$$a = \frac{0.45724 r_{\mathrm{c}}^2 p_{\mathrm{c}}^2}{0.55T_{\mathrm{c}}} \tag{3}$$

$$b = \frac{0.07780 r_{\mathrm{c}} p_{\mathrm{c}}}{0.55T_{\mathrm{c}}} \tag{4}$$

$$r' = \beta r_{\mathrm{c}} \tag{5}$$

where the variables in Eqs. (3), (4) and (5) can be obtained from the following expressions:

$$\beta = e_0(1 - p_r^{-1}) - 0.02715 p_r^{-1}[(p_r + 0.25)^{-1} - 0.8] + p_r^{-1} \tag{6}$$

$$e_0 = 0.03192 - 3.3125\times10^{-4}\omega M_w \tag{7}$$

$$r_{\mathrm{c}} = \frac{0.55\mu_{\mathrm{c}} T_{\mathrm{c}}}{p_{\mathrm{c}} Z_{\mathrm{c}}} \tag{8}$$

where $p_r = \dfrac{p}{p_{\mathrm{c}}}$ is the reduced pressure; Z_{c} is the critical compressibility factor equal to 0.3074 commonly ; $\mu_{\mathrm{c}} = 7.7T_{\mathrm{c}}^{-1/6} M_w^{0.5} p_{\mathrm{c}}^{2/3}$ indicate the critical viscosity.

Xia et al. [29] proved that, by replacing the constant 0.3074 with the real critical compressibility factor to solve r_c in Eq. (8), a more accurate viscosity value of each component could be obtained. Meanwhile, they found that the binary interaction coefficient had little effect on the viscosities of gas and liquid phase.

To improve the accuracy of EOS, imitating the volume-translated Peng-Robinson (VTPR) EOS, Fan and Wang [6] defined a correction of viscosity as volume-translated Peng-Robinson viscosity (VTPRμ) equation, which is given as:

$$\mu^{\mathrm{VTPR}} = \mu^{\mathrm{PR}} + c_0 + c \tag{9}$$

where μ^{VTPR} and μ^{PR} are the viscosity corrected by volume translation and calculated by Eq. (1), respectively, 10^{-7} Pa·s; c_0 and c denote correction terms, and the detailed solution method can be found in Ref [6].

In order to extend the VTPRμ EOS to prediction of mixture viscosity precisely, an improved one parameter van der Waals mixing rule proposed by Khosharay [30] is adopted. That is:

$$z_m = \sum_i \sum_j x_i x_j z_{ij} \ \ , \ \ z = a, b, r_c, T_d \ \text{ and } \ \beta \tag{10}$$

$$c_m = \sum_i x_i c_i \tag{11}$$

where

$$z_{ij} = \sqrt{z_i z_j} \tag{12}$$

In this study, the corresponding relationship among the fluid temperature, pressure and the ratio of each component in the flow process, can be derived by the phase equilibrium calculation [2] based on VTPR EOS [31] with classical one parameter van der Waals mixing rule [32]. The method on pure component properties used to calculate the parameters of VTPR EOS and the binary interaction parameters could be found from Ref. [33]. Then, for an improvement of calculation results, the average viscosity μ_{tp} of two-phase mixture under different pressures can be obtained using the above VTPRμ EOS associated with improved mixing rule. There are six common formulae for calculating viscosity of mixture in the opening literature, as shown in Table 1, and thus six corresponding methods (VM-1 to VM-6) can be established for calculating the average viscosity.

Table 1 Common calculation methods of average viscosity of fluid mixture

Abbreviation	Formula	Literature
VM-1	$\mu_{\mathrm{tp}} = (\frac{x}{\mu_v} + \frac{1-x}{\mu_l})^{-1}$	McAdams et al. [34]
VM-2	$\mu_{\mathrm{tp}} = x\mu_v + (1-x)\mu_l$	Cicchitti et al. [35]

VM-3	$\mu_{\text{tp}} = \rho_{\text{tp}}[\frac{x\mu_v}{\rho_v} + (1-x)\frac{\mu_l}{\rho_l}]$	Dukler et al. [36]
VM-4	$\mu_{\text{tp}} = \mu_l - 2.5\mu_l[\frac{x\rho_l}{x\rho_l + (1-x)\rho_v}]^2 + [\frac{x\rho_l(1.5\mu_l + \mu_v)}{x\rho_l + (1-x)\rho_v}]$	Beattie-Whalley [37]
VM-5	$\mu_{\text{tp}} = \frac{\mu_v\mu_l}{\mu_g + x^{1.4}(\mu_l - \mu_v)}$	Lin et al. [38]
VM-6	$\mu_{\text{tp}} = \mu_v \frac{2\mu_v + \mu_l - 2(\mu_v - \mu_l)(1-x)}{2\mu_v + \mu_l + (\mu_v - \mu_l)(1-x)}$	Awad-Muzychka [39]

2.2 Steady-state two-phase flow model

2.2.1 Steady-state two-phase flow equations

As mentioned earlier, few detailed available studies on the steady-state two-phase flow of nitrogen + extinguishant in a pipeline have been discussed, while the gas-liquid two-phase flow of refrigerant in a capillary tube has been sufficiently studied. As the refrigerant enters the capillary tube, it is generally assumed that the two-phase flow is stable in straight pipe. This provides a reference for the large mass flux two-phase flow of nitrogen + extinguishant in the pipeline.

Next, the control equations of two-phase flow in the pipe are established based on the homogeneous flow model.

(1) Continuous equation

For the mixture of nitrogen and fire extinguishing agent, at a constant pipeline diameter d, the steady-state flow continuous equation is as follows:

$$G = \rho_{\text{m}} u = const \tag{13}$$

where: u denotes the velocity of two-phase flow, m·s^{-1}; ρ_{m} is the average density of mixture, represented by the following formula:

$$\rho_{\text{m}} = (\frac{x}{\rho_{\text{v}}} + \frac{1-x}{\rho_{\text{l}}})^{-1} \tag{14}$$

where: ρ_{v} is the average density of nitrogen and agent vapor in vapor phase, while ρ_{l} is the average density of nitrogen and agent in liquid phase, and they could be calculated based on the VTPR equation and one parameter van der Waals mixing rule.

(2) Momentum equation

The momentum equation [40] in the homogeneous flow model can be written as the sum of three pressure drop gradients, as follows:

$$-\frac{dp}{dL}=\frac{dp_f}{dL}+\frac{dp_a}{dL}+\frac{dp_g}{dL} \tag{15}$$

where: $\frac{dp_f}{dL}$ is the pressure gradient due to friction; $\frac{dp_a}{dL}$ is the pressure gradient due to acceleration; $\frac{dp_g}{dL}$ is the pressure gradient due to gravity, which is generally ignored because of horizontal straight pipe.

$\frac{dp_f}{dL}$ in Eq. (15) can be acquired through analogy with the calculation method on a single-phase flow:

$$\frac{dp_f}{dL}=\lambda\frac{1}{d}\times\frac{1}{2}\rho_m u^2=\frac{2f\rho_m u^2}{d}=\frac{2fG^2}{d\rho_m} \tag{16}$$

where: f denotes friction factor, and is calculated as follows [41]:

$$f=0.25[\log(\frac{150.39}{Re^{0.98865}}-\frac{152.66}{Re})]^{-2} \tag{17}$$

The definition of Reynolds number Re is as follows:

$$Re=\frac{\rho_m ud}{\mu_{tp}}=\frac{Gd}{\mu_{tp}} \tag{18}$$

where: μ_{tp} is the average viscosity of binary mixture, calculated by methods (VM-1 to VM-6) given in Table 1, Pa·s.

$\frac{dp_a}{dL}$ in Eq. (15) expresses the acceleration pressure drop gradient, defined as:

$$\frac{dp_a}{dL}=G^2\frac{d}{dL}[\frac{x^2}{\rho_v\beta}+\frac{(1-x)^2}{\rho_l(1-\beta)}]=G^2\frac{d(1/\rho_m)}{dL} \tag{19}$$

Combining Eqs. (15), (16), and (19), yields a differential equation of momentum as follows：

$$udu+\frac{dp}{\rho_m}+\frac{2fu^2}{d}dL=0 \tag{20}$$

Adding a multiplier ρ_m^2 to both sides of Eq. (20), introducing the formula of continuous Eq. (13), and integrating the pipeline with length *L* and diameter *d*, the following equation is obtained:

$$\int_{p_1}^{p_2} \rho_m dp + G^2 \ln(\frac{\rho_1}{\rho_2}) + \frac{2fG^2L}{d} = 0 \tag{21}$$

where p_1, ρ_1, p_2, and ρ_2 are the inlet pressure, inlet density, outlet pressure and outlet density of mixture along the pipe section, respectively.

(3) Energy equation

The heat exchange between the wall and the fluid can be ignored due to the very short flowing time through the pipeline. Consequently, it could be assumed that the two-phase fluid undergoes the adiabatic isenthalpic expansion process in the pipeline. Finally, the energy equation can be described as follows:

$$\frac{dh_0}{dL} = 0 \tag{22}$$

where: h_0 is stagnation enthalpy, calculated as follows:

$$h_0 = h + u^2/2 = x_\mathrm{v}^\mathrm{N} h_\mathrm{v}^\mathrm{N} + x_\mathrm{v}^\mathrm{E} h_\mathrm{v}^\mathrm{E} + x_\mathrm{l}^\mathrm{N} h_\mathrm{l}^\mathrm{N} + x_\mathrm{l}^\mathrm{E} h_\mathrm{l}^\mathrm{E} + u^2/2 \tag{23}$$

where: the superscripts N and E are divided into nitrogen and fire extinguishing agent, and *x* is the quality of the corresponding component.

Since VM-1 to VM-6 are used to calculate Reynolds number, the six corresponding steady-state two-phase flow models are proposed, named STFM-1 to STFM-6.

2.2.2 Solution of mathematical model

The continuity and momentum equations describing the steady-state two-phase flow of nitrogen + extinguishant in the pipeline are both concentrated in Eq. (21). In this study, the nitrogen + extinguishant undergoes adiabatic isenthalpic expansion with two degrees of freedom. Specific enthalpy *h* and total pressure *p* are selected as two independent variables. Considering VTPR EOS with one parameter van der Waals mixing rule and constant specific enthalpy, the state parameters of mixture and each component are calculated iteratively. Furthermore, the density of mixture is explicitly indicated by the pressure along the pipeline, and the relationship between mass velocity *G* and total pressure *p* can be obtained through direct integration of Eq. (21).

As mentioned earlier, it is usually believed that the "front end" (the part in contact with the outside) of the extinguishing agent filling the pipeline will reach the critical flow state of two-phase if the fire extinguishing system is opened [3, 4]. At this moment, the mass velocity G in the pipeline reaches the maximum value in spite of the decrease of the outlet pressure. Referring to the typical calculation method of the gas-liquid two-phase critical flow in a capillary [16], the procedure to solve the continuity equation, momentum equation and energy equation of the steady-state two-phase flow is shown below:

(1) According to the given initial filling pressure (p_0) and temperature (T_0,), mass of the fire extinguishing agent (m^E), volume of the fire extinguishing bottle (V_b), and diameter (d) and length (L) of pipeline, the values for mass of dissolved nitrogen (m^N) can be acquired by solving initial state.

(2) Obtain $\rho_m = \rho_m(p)$ in adiabatic isenthalpic expansion process based on foregoing method mentioned.

(3) Assume initial mass velocity G_0.

(4) Provide pressure drop of control body dp.

(5) Calculate the pressure outside the pipeline p_2 by Eq. (21).

(6) Compare the calculated mass flow rate G and stop the calculation when the condition $G = G_{max}$ is met, otherwise recalculate G by using the second method and go to step 4 for iterative calculation.

3 Results and discussion

In this section, the representative physical parameters (average viscosity and density) and key flowing properties (mass flow rate and pressure drop) are calculated and predicted. Following that, the accuracy of six viscosity methods (VM-1 to VM-6) and corresponding steady-state two-phase flow models (STFM-1 to STFM-6) for nitrogen + extinguishant are evaluated against the data from the published literature.

3.1 Physical parameters

3.1.1 Average viscosity

The results of the average viscosity for different mixtures calculated by VM-1 to VM-6 are compared with that from National Institute of Standards and Technology (NIST) [4] at a different filling pressure p_0, as presented in Figs. 2-3. The fire extinguishing agents are HFC227ea and HFC125.

Among all mixtures, there is a similar upward trend for average viscosity of the two-phase flow through adiabatic isenthalpic expansion calculated by the above methods except VM-2 and VM-4. Taken together, the average viscosities calculated by VM-1 and VM-3 are close to that from Ref. [4], while quite different from results of VM-2 and VM-4.

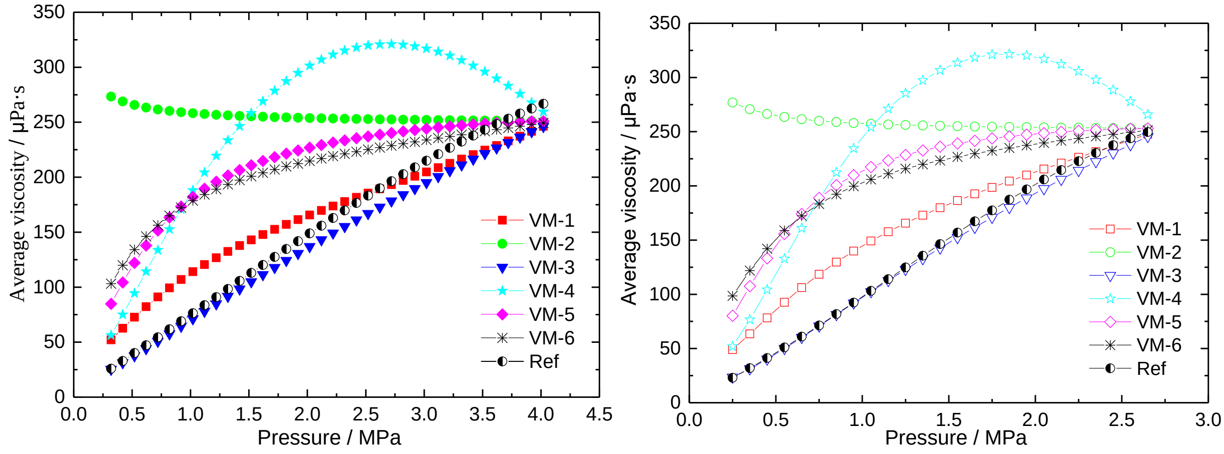

(a) p_0 = 4.12 MPa (b) p_0 = 2.75 MPa

Fig. 2 Comparison of N_2 + HFC227ea average viscosities at different p_0

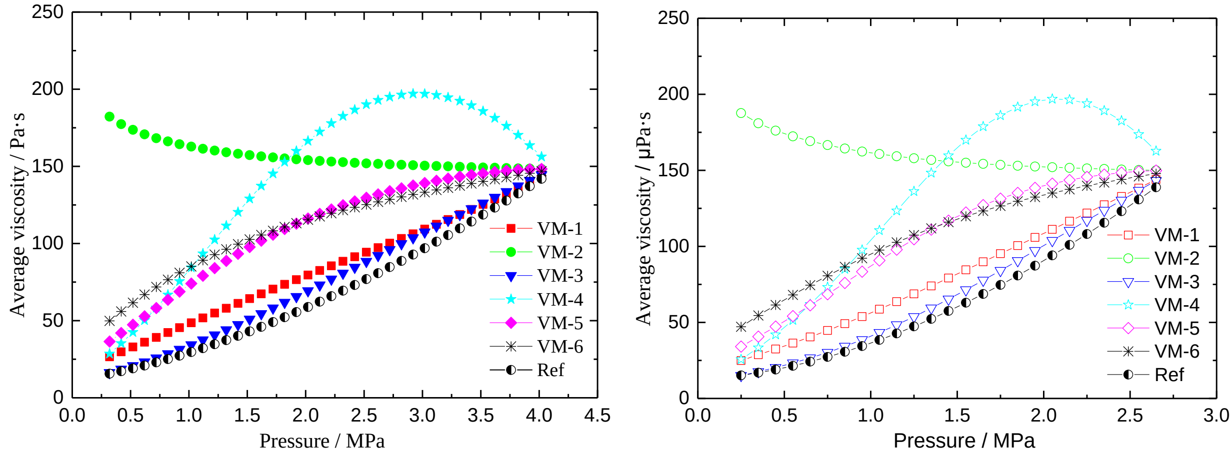

(a) p_0 = 4.12 MPa (b) p_0 = 2.75 MPa

Fig. 3 Comparison of N_2 + HFC125 average viscosities at different p_0

However, it is difficult to directly determine which calculation formula is more suitable for calculating the Reynolds number of a gas-liquid two-phase flow only by the trend of average viscosity calculation for nitrogen + extinguishant. Furthermore, it has been reported in literature [42, 43] that VM-2 could obtain the best description value of pressure drop in homogeneous flow model, while in Ref. [44] VM-3 could relatively reasonably predict the experimental data. Therefore, the mass flow rate and pressure drop of a steady-state two-phase flow are further studied in the following section.

3.1.2 Average density

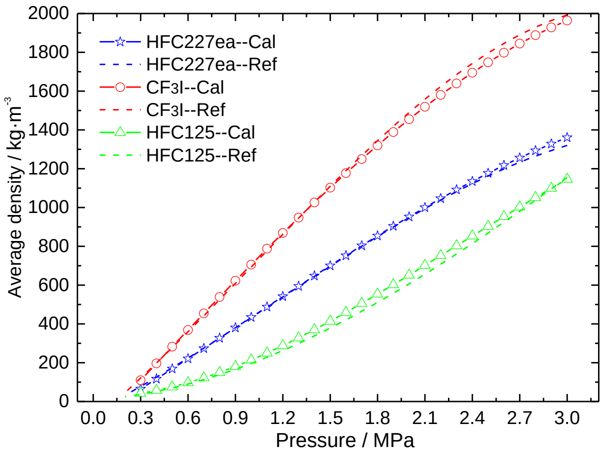

(a) p_0 = 3.0 MPa

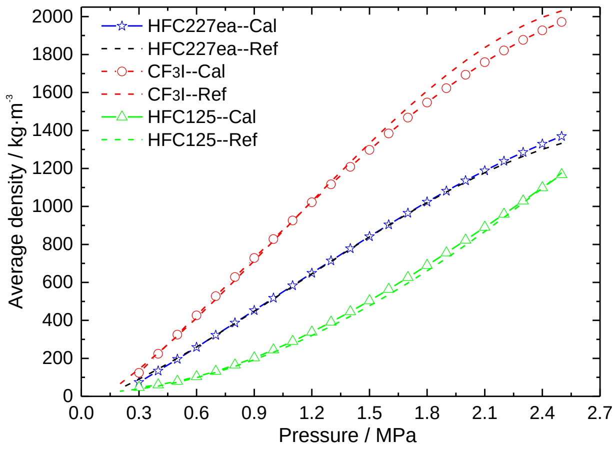

(b) p_0= 2.5 MPa

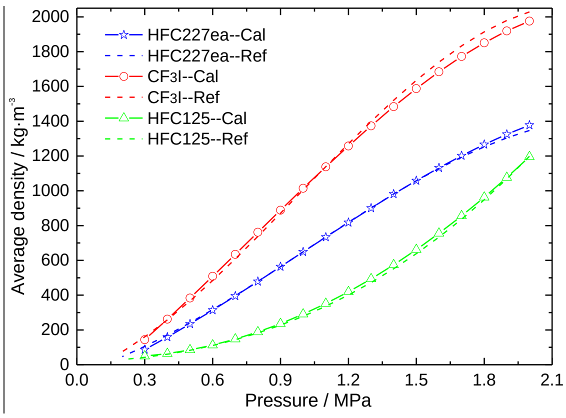

(c) p_0 = 2.0 MPa

Fig. 4 Curves of the average densities of two-phase mixtures with pressure

As another key parameter in the steady-state two-phase models, the densities of three types of mixtures are determined based on VTPR EOS with one parameter van der Waals mixing rule. Fig. 4 shows that the average densities vary with the pressure through adiabatic isenthalpic expansion. The mixtures are N_2 + HFC227ea, N_2 + CF_3I, and N_2 + HFC125, respectively. The initial filling temperature T_0 in the fire extinguisher is 23 °C and the initial filling pressures p_0 are 3.0 MPa, 2.5 MPa, and 2.0 MPa, respectively.

At p_0 = 3.0 MPa, the average relative deviations (ARDs) of densities of the three binary mixtures calculated in this study against the Ref. [4] are 1.75%, 2.13%, 6.92%, and 5.12%, while 1.88%, 3.20%, 5.38%, and 4.20% at 2.5 MPa, and 1.97%, 3.08%, 3.88%, and 3.47% at 2.0 MPa, respectively. It can be found that all the average densities of mixtures decrease as the fluid pressure declines at different initial filling pressures, and the predicted values are markedly consistent with the quoted values. Therefore, the calculated average densities are adopted to predict the two-phase mass flow rate and pressure drop of nitrogen + extinguishant.

In order to simplify the solution of steady-state two-phase flow equations, the average density of each two-phase mixture is fitted to a univariate cubic polynomial with pressure, as shown in Eq. (24).

$$\rho_{\mathrm{m}} = A_0 + A_1 \cdot p_{\mathrm{m}} + A_2 \cdot p_{\mathrm{m}}^{\ 2} + A_3 \cdot p_{\mathrm{m}}^{\ 3} \tag{24}$$

where: ρ_{m} is the average density of mixture, kg·m^{-3}; p_{m} is the pressure of mixture, MPa; A_0 - A_3 are the polynomial coefficients of the pressure.

The fitted polynomial coefficients for three binary mixtures under three initial filling pressures are reported in Table 2.

Table 2 The polynomial coefficients under different initial filling pressures

Agent	p_0 /MPa	A_0	A_1	A_2	A_3
	3.0	-83.181	479.941	55.936	-18.502
HFC227ea	2.5	-93.304	523.914	129.194	-41.882
	2.0	-98.020	525.882	335.768	-114.915
	3.0	-150.586	864.999	13.490	-22.280
CF_3I	2.5	-168.524	948.824	104.015	-56.462
	2.0	-176.917	965.843	395.573	-170.137
HFC125	3.0	21.596	7.400	216.577	-31.370
	2.5	42.062	-75.301	322.822	-45.017

	2.0	46.242	-90.322	337.099	-2.241

3.2 Calculation and comparison of steady-state two-phase flow

The mass flow rate and pressure drop, as the key flowing properties of steady-state two-phase nitrogen + extinguishant, are predicted and then compared with calculated and experimental data from the opening literature.

3.2.1 Mass flow rate

Table 3 compares the steady-state mass flow rates of nitrogen + extinguishant predicted by STFM-1 to STFM-6 and measured by Yang et al. [4]. For the three types of mixtures, the STFM-3 and STFM-4 always show the largest and smallest mass flow rate respectively, at the same filling pressure and pipeline diameter. However, there is not much obvious difference among the results of the six models.

Table 3 Steady-state mass flow rate of two-phase mixture

Agent	p_0 /MPa	T_0 /°C	d /mm	Mass flow rate [4] / kg·s^{-1}	Calculated mass flow rate / kg·s^{-1}					
					STFM-1	STFM-2	STFM-3	STFM-4	STFM-5	STFM-6
HFC227ea	3.0	23	9.5	1.58±0.02	1.7981	1.7744	1.8104	1.7556	1.7793	1.7834
	2.5	23	9.5	1.51±0.02	1.4723	1.4436	1.4879	1.4284	1.4506	1.4548
	2.0	23	9.5	1.32±0.01	1.1461	1.1145	1.1642	1.1083	1.1239	1.1274
	3.0	23	15.9	5.37±0.21	5.8599	5.8019	5.8888	5.7466	5.8128	5.8238
	2.5	23	15.9	5.13±0.18	4.7868	4.7142	4.8255	4.6661	4.7304	4.7422
	2.0	23	15.9	5.25±0.19	3.7223	3.6407	3.7688	3.6169	3.6633	3.6733
CF_3I	3.0	23	9.5	1.97±0.02	2.2495	2.2246	2.2665	2.2012	2.2289	2.2339
	2.5	23	9.5	1.83±0.02	1.8530	1.8231	1.8744	1.8028	1.8290	1.8344
	2.0	23	9.5	1.52±0.01	1.4522	1.4189	1.4770	1.4082	1.4270	1.4319
	3.0	23	15.9	7.00±0.29	7.3633	7.3021	7.4039	7.2334	7.3119	7.3248

	2.5	23	15.9	6.83±0.29	6.0459	5.9699	6.0992	5.9073	5.9839	5.9984
	2.0	23	15.9	6.53±0.27	4.7304	4.6442	4.7941	4.6071	4.6637	4.6775
	3.0	23	9.5	1.29±0.02	1.4667	1.4403	1.4716	1.4257	1.4488	1.4511
	2.5	23	9.5	1.10±0.01	1.1554	1.1223	1.1624	1.1139	1.1355	1.1367
HFC125	2.0	23	9.5	1.13±0.01	0.8591	0.8233	0.8676	0.8264	0.8411	0.8402
	3.0	23	15.9	4.38±0.18	4.7203	4.6575	4.7310	4.6132	4.6754	4.6825
	2.5	23	15.9	4.50±0.16	3.7101	3.6275	3.7269	3.5976	3.6579	3.6625
	2.0	23	15.9	3.30±0.11	2.7547	2.6629	2.7761	2.6645	2.7065	2.7054

The comparison between the predicted and the experimental values is completed and presented in Fig. 5. When d is 9.5 mm, the results predicted by six models correspond to the experimental values within a percent deviation smaller than 15% under all operational conditions. For STFM-1 to STFM-6, the average absolute relative deviation (AARD) between predicted and experimental data is 8.94%, 8.93%, 8.86%, 8.74%, 8.82%, and 8.87%, respectively. Nevertheless, the deviations exceed ±15% as d increases to 15.9 mm under some conditions, and the corresponding AARD is 14.1%, 14.92%, 13.77%, 14.93%, 14.58% and 14.56%, respectively.

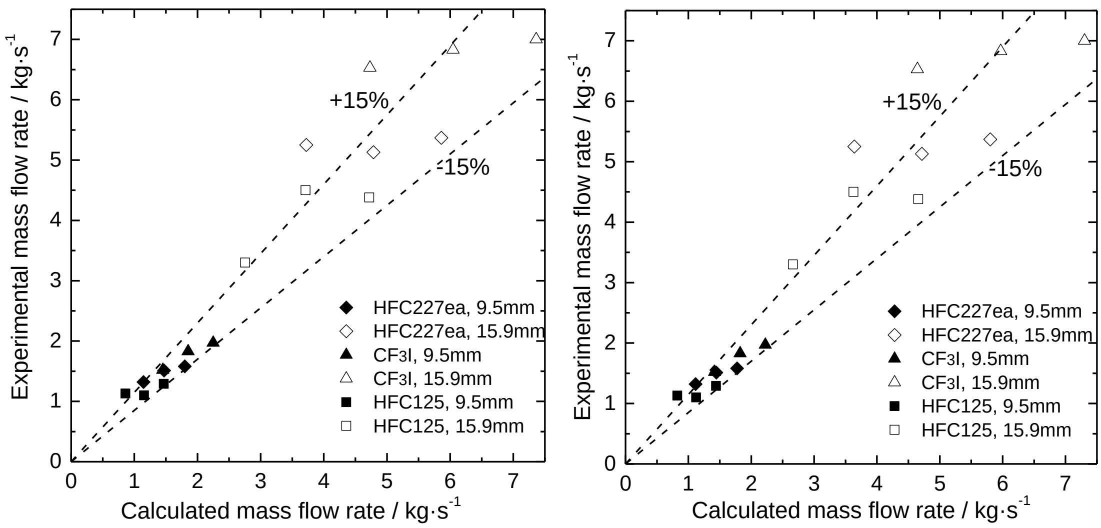

(a) STFM-1 (b) STFM-2

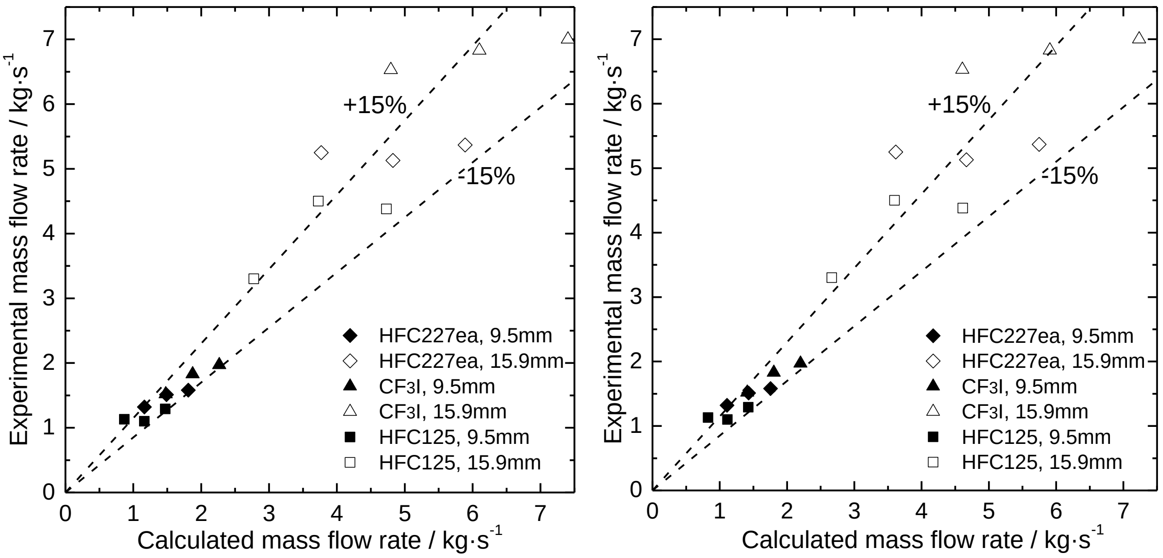

(c) STFM-3 (d) STFM-4

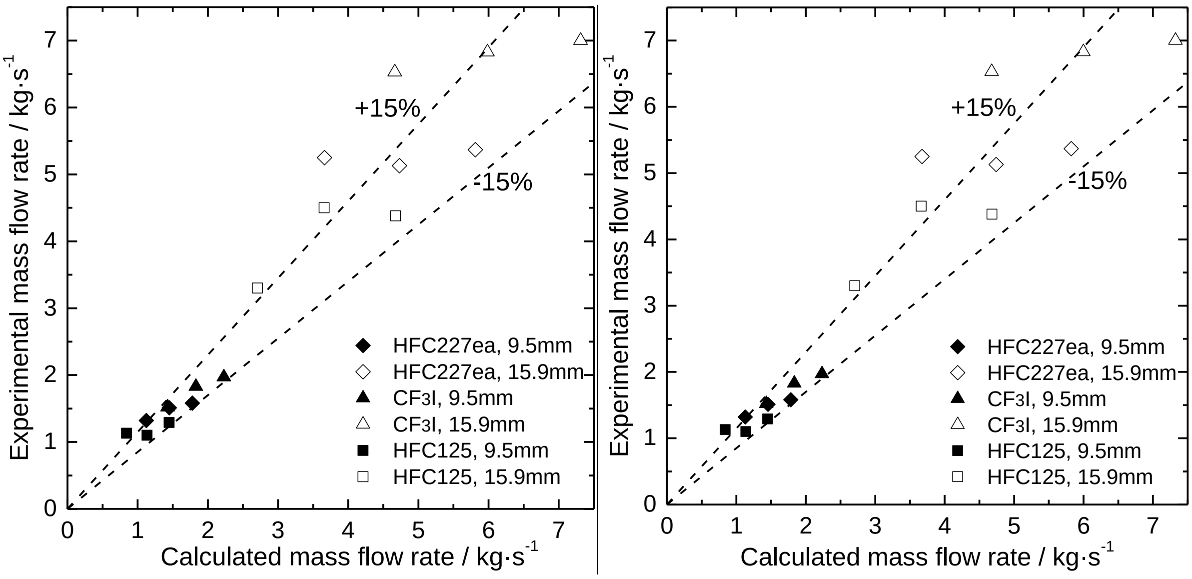

(e) STFM-5 (f) STFM-6

Fig. 5 Comparison between the predicted and experimental value [4] of steady-state mass flow rate

In comparison with the experimental data, different models have various calculation accuracy for each mixture. For HFC227ea, CF_3I, and HFC125, the appropriate prediction models are STFM-3, STFM-2, and STFM-2, respectively. However, the predicted mass flow rate results based on different models are mainly desirable, especially with a small pipeline diameter, and they all can calculate viscosity in homogeneous flow model.

For predicting the mass flow rate through the fire extinguishing pipeline conveniently, a dimensionless criterion correlation is proposed. Referring to Buckingham's π theorem [13, 14] and the selection of variables from Ref. [13], the specific forms are as follows:

$$\pi_1 = \phi(\pi_2, \pi_3, \pi_4, \pi_5, \pi_6) \tag{25}$$

$$\frac{\dot{m}}{d^2\sqrt{\rho_l p_0}} = \phi(\frac{p_0}{p_c}, \frac{T_0}{T_c}, \frac{L}{d}, \frac{\rho_v}{\rho_l}, \frac{\mu_l - \mu_v}{\mu_g}) \tag{26}$$

where: $\dot{m}$ is the mass flow rate, kg·s^{-1}; μ_v and μ_l are the dynamic viscosity of gas mixture and liquid fire extinguishing agent of dissolved nitrogen respectively, Pa·s.

The function form of power law is suitable for this study [13], and the coefficients in Eq. (26) are optimised by the 'Nlinfit' function from MATLAB software [45]. Finally, the best mass flow rate correlation can be expresses as follows:

$$\frac{\dot{m}}{d^2\sqrt{\rho_l p_0}} = 2.3645\times10^{-5}(\frac{p_0}{p_c})^{0.3859}(\frac{T_0}{T_c})^{-10.6972}(\frac{L}{d})^{2.2925}(\frac{\rho_v}{\rho_l})^{-0.0310}(\frac{\mu_l - \mu_v}{\mu_v})^{-2.2675} \tag{27}$$

The developed correlation for mass flow rate shows good agreement with the experimental data with an overall ARD of 1.43%, covering HFC227ea, CF_3I, and HFC125.

N_2 + FC218 is selected as a new two-phase mixture to further evaluate the applicability of correlation. The mass flow rate of a steady-state two-phase flow is calculated by the correlation and STFM-2, and the comparison result is shown in Table 4. The value calculated by Eq. (27) is lower than that by selected prediction model as a whole, with all deviations of no more than 10% at different p_0 and d, indicating that the correlation has a satisfying applicability and accuracy.

Table 4 Comparison of mass flow rate of N_2 + FC218

	p_0 /MPa	d /mm	STFM-2 / kg·s^{-1}	Correlation / kg·s^{-1}	Deviation
1	3.0	9.5	1.639	1.537	-6.22%
2	2.5	9.5	1.307	1.199	-8.26%
3	2.0	9.5	0.984	0.886	-9.96%
4	3.0	15.9	5.340	5.004	-6.29%
5	2.5	15.9	4.245	3.904	-8.03%
6	2.0	15.9	3.194	2.886	-9.64%

3.2.2 Pressure drop

In this section, the pressure drops of two-phase nitrogen + extinguishant mixtures flowing along the pipeline are predicted and discussed, including HFC227ea, CF_3I, and HFC125, and further compared with the experimental and calculated values in Ref. [4].

Fig. 6 (a) and (b) illustrate the predicted and experimental pressure change of the two-phase N_2 + HFC227ea at several measuring points along the pipeline, where the downward pressure tendency is similar for the other mixtures. Here, STFM-3 is adopted to predict pressure which decreases as the fluid gradually flows forward. At d = 9.5 mm, the pressure drops predicted in this article are all quite consistent with the previous data at three initial filling pressures. As d increases to 15.9 mm, the predicted value corresponds to the calculated value within 2.6 m from the pipeline inlet, while differs from that beyond 3.6 m. The predicted result is evidently closer to the experimental data than the calculation, which indicates better prediction ability of STFM-3.

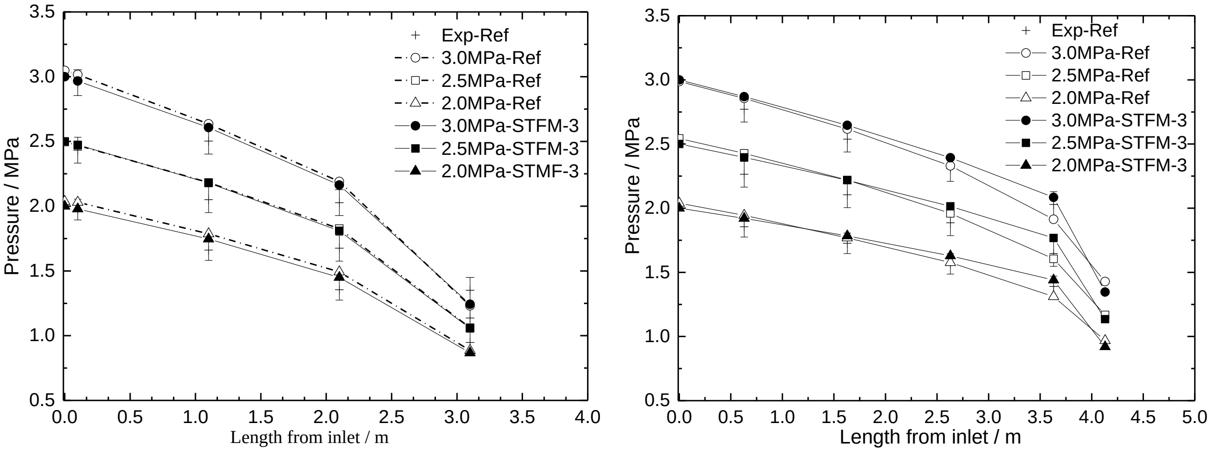

(a) d = 9.5 mm (b) d = 15.9 mm

Fig. 6 Comparison between predicted and experimental data of two-phase N_2 + HFC227ea pressure drop

Tables 5-7 present pressure drop with high value predicted by six models and quoted from Ref. [4] at different p_0 and d, for N_2 + HFC227ea, N_2 + CF_3I, and N_2 + HFC125, respectively. Compared with the experimental data for the types of mixtures, most ARDs calculated by STFM-1 to STFM-6 are approximately 10%, versus about 20% given by literature, which reveals that these models are more appropriate for the two-phase pressure drop.

Specifically, the calculation values for pressure drop of Ref. [4] are close to that of the six models at small pipe diameter of 9.5 mm, while the deviations of quoted data are significantly higher than that of prediction models as diameter increases to 15.9 mm. Considering the predicted accuracy of STFM-1 to STFM-6 synthetically, STFM-2 is the most accurate prediction model for pressure drop, which corresponds to the views of literature [42, 46], followed by STFM-4.

Table 5 Steady-state flow pressure drop of two-phase N_2 + HFC227ea

	p_0 /MPa	d /mm	Pressure drop / MPa Exp [4]	Cal [4]	STFM-1	STFM-2	STFM-3	STFM-4	STFM-5	STFM-6
1	3.0	9.5	1.603	1.786	1.713	1.699	1.724	1.725	1.707	1.706
2	2.5	9.5	1.296	1.409	1.411	1.405	1.416	1.438	1.412	1.409
3	2.0	9.5	1.025	1.145	1.113	1.111	1.112	1.143	1.119	1.115
4	3.0	15.9	0.743	0.943	0.818	0.785	0.836	0.758	0.791	0.797
5	2.5	15.9	0.617	0.822	0.670	0.629	0.695	0.607	0.638	0.644
6	2.0	15.9	0.465	0.633	0.526	0.480	0.557	0.470	0.493	0.498
	ARD %			21.35	9.35	5.60	11.71	5.80	6.75	7.11

Note: pressure drop refers to the pressure difference between measuring points 1 and 4 [4], similarly hereinafter.

Table 6 Steady-state flow pressure drop of two-phase N_2 + CF_3I

	p_0 /MPa	d /mm	Pressure drop / MPa Exp [4]	Cal [4]	STFM-1	STFM-2	STFM-3	STFM-4	STFM-5	STFM-6
1	3.0	9.5	1.574	1.749	1.755	1.743	1.767	1.764	1.748	1.748
2	2.5	9.5	1.468	1.419	1.441	1.434	1.448	1.464	1.440	1.438
3	2.0	9.5	1.089	1.026	1.132	1.130	1.133	1.158	1.135	1.133
4	3.0	15.9	0.761	0.988	0.849	0.821	0.869	0.794	0.825	0.831
5	2.5	15.9	0.545	0.808	0.693	0.658	0.719	0.634	0.664	0.671
6	2.0	15.9	0.434	0.624	0.541	0.502	0.574	0.489	0.511	0.517
	ARD %			23.68	13.44	10.18	16.01	8.67	10.86	11.43

Table 7 Steady-state flow pressure drop of two-phase N_2 + HFC125

	p_0	d	Pressure drop / MPa

	/MPa	/mm	Exp [4]	Cal [4]	STFM-1	STFM-2	STFM-3	STFM-4	STFM-5	STFM-6
1	3.0	9.5	1.351	1.364	1.453	1.434	1.459	1.467	1.451	1.445
2	2.5	9.5	1.012	1.062	1.203	1.199	1.207	1.242	1.214	1.206
3	2.0	9.5	0.887	0.792	0.967	0.975	0.966	1.011	0.984	0.977
4	3.0	15.9	0.608	0.753	0.666	0.626	0.674	0.604	0.638	0.642
5	2.5	15.9	0.382	0.602	0.546	0.494	0.559	0.479	0.513	0.515
6	2.0	15.9	0.351	0.483	0.435	0.374	0.452	0.377	0.401	0.400
		ARD %		22.61	18.64	12.23	20.36	13.13	15.30	15.11

Even though many studies have proposed correlations of frictional pressure drop based on the data of an adiabatic two-phase flow [18, 47-50], there have been few studies on the nitrogen + extinguishant in pipeline with large mass flow rate. Therefore, in this paper, the frictional pressure drop correlation is proposed for extinguishant consulting previous models according to predicted data using the two-phase multiplier ϕ_{vo}^2 and frictional pressure drop for a vapor phase with total flow $\left(\frac{dp}{dz}\right)_{\mathrm{vo}}$. The proposed correlation is given as:

$$\left(\frac{\mathrm{dp}}{\mathrm{dz}}\right)_{\mathrm{tp}} = \left(\frac{\mathrm{dp}}{\mathrm{dz}}\right)_{\mathrm{vo}} \phi_{\mathrm{vo}}^2 \tag{28}$$

$$\left(\frac{dp}{dz}\right)_{\mathrm{vo}} = \frac{2 f_{vo} G^2}{d \rho_v} \tag{29}$$

$$\phi_{vo}^2 = x^{1.8} + (1-x)^{1.8} \frac{\rho_v f_{lo}}{\rho_l f_{vo}} + 0.68 x^{0.71} (1-x)^{0.50} \left(\frac{\mu_l}{\mu_v}\right)^{1.76} \left(\frac{\rho_l}{\rho_v}\right)^{0.62} \tag{30}$$

where Jige [49] suggested a correlated method with friction factor f using the vapor Reynolds number.

The comparison suggests that the developed correlation is able to work for the mass flow rates of nitrogen + extinguishant accurately with an overall ARD of 1.43%, covering HFC227ea, CF_3I, and HFC125.

4 Conclusions

The purpose of the current research is to analyse and study the steady-state two-phase flow performance of nitrogen + extinguishant in a pipeline accurately, including N_2 + HFC227ea, N_2 + CF_3I, and N_2 + HFC125. Based on the VTPRμ EOS associated with improved mixing rule in the opening literature, the flow process viewed as one-dimensional adiabatic isenthalpic expansion is studied. The average viscosities and densities are calculated and discussed as significant physical parameters. The novel steady-state two-phase flow models (STFM-1 to STFM-6) with large mass flux for the mass flow rate and pressure drop are proposed and evaluated, which correspond to the six collected mixture viscosity formulae (VM-1 to VM-6). The major conclusions are summarized as follows:

Among all mixtures in the paper, there is a similar rising trend for average viscosity except VM-2 and VM-4. Moreover, the average density of each two-phase mixture decreases with the pressure loss at different initial filling pressure, which is further fitted to a univariate cubic polynomial.

For mass flow rate, the results calculated by STFM-1 to STFM-6 are generally satisfactory compared with the previous experimental values, especially for a small pipeline diameter, thus they all can be utilised to predict mass flow rate of nitrogen + extinguishant. The most appropriate models are STFM-3, STFM-2, and STFM-2, respectively, corresponding to HFC227ea, CF_3I, and HFC125. A dimensionless correlation for mass flow rate is established and yields an overall ARD of 1.43%, which can also be extended to accurately predict that of N_2 + FC218.

For pressure drop, STFM-2 has the most adequate calculation accuracy under different initial filling pressure and pipeline diameter for each nitrogen + extinguishant above, followed by STFM-4. In addition, for all flow conditions a correlation is newly developed and works satisfactorily for frictional pressure drop with an ARD of 6.15%.

In general, the insights gained from this study will be invaluable for large mass flux steady-state two-phase flow process analysis.

References

[1] Zhang T, Liu H, Han Z, Wang Y, Guo Z, Wang C. Experimental study on the synergistic

effect of fire extinguishing by water and potassium salts. J Therm Anal Calorim. 2019; 138: 857–867.

[2] Liu S, Xie Y, Chen M, Zhu J, Day R, Wu H, Yu J. Prediction of the release process of the nitrogen-extinguishant binary mixture considering surface tension. J Therm Anal Calorim. 2020; 1-15.

[3] Grosshandler W L, Gann R G, Pitts W M. Evaluation of alternative in-flight fire suppressants for full-scale testing in simulated aircraft engine nacelles and dry bays. NIST SP-861, Washington DC. 1994.

[4] Yang J C, Cleary T G, Vázquez I, Boyer C I, King M D, Breuel B D, Gmurczyk G. Optimization of system discharge. In: Fire suppression system performance of alternative agents in aircraft engine and dry bay laboratory simulations, NIST SP-890, Washington DC. 1995; pp 407-782.

[5] Wang L S, Lv H C. A unified model for representing densities and viscosities of hydrocarbon liquids and gases based on Peng-Robinson equation of state. Open Thermodynamics Journal. 2009; 3(1): 24-33.

[6] Fan T B, Wang L S. A viscosity model based on Peng–Robinson equation of state for light hydrocarbon liquids and gases. Fluid Phase Equilib. 2006; 247(1): 59-69.

[7] Tuzla K, Palmer T, Chen J C, Sundaram R K, Yeung W S. Development of computer program for fire suppressant fluid flow. Lehigh University, Bethlehem. 2000.

[8] Vacek V, Vinš V. Two-phase flow analyses during throttling processes. Int J Thermophys. 2009; 30(4): 1179-1196.

[9] Vinš V, Hrubý J, Vacek V. Numerical simulation of gas-contaminated refrigerant two-phase flow through adiabatic capillary tubes. Int J Heat Mass Transf. 2010; 53(23): 5430-5439.

[10] Mehdi R, Jeong H, Ji H. Development of a continuous empirical correlation for refrigerant mass flow rate through non-adiabatic capillary tubes. Appl Therm Eng. 2017; 127: 547-558.

[11] Jadhav, Pravin, Agrawal, Neeraj. Study of Homogenous Two Phase Flow Through Helically Coiled Capillary Tube. Adv Sci. 2018; 10(3):513-517.

[12] Mehdi R, Ji H. A generalized continuous empirical correlation for predicting refrigerant mass flow rates through adiabatic capillary tubes. Appl Therm Eng. 2018; 139:47-60.

[13] Nilpueng K, Wongwises S. Choked flow mechanism of HFC134a flowing through short-tube orifices. Exp Therm Fluid Sci. 2011; 35(2): 347-354.

[14] Shao L L, Wang J C, Jin X C, Zhang C L. Assessment of existing dimensionless correlations of refrigerant flow through adiabatic capillary tubes. Int J Refrig. 2013; 36(1): 270-278.

[15] Masoud Z, Morteza K, Hamed F. Numerical simulation of two phase refrigerant flow through non-adiabatic capillary tubes using drift flux model. J Mech Sci Technol. 2018; 32: 381-389.

[16] Deodhar S D, Kothadia H B, Iyer K N, Iyer K N, Prabhu S V. Experimental and numerical studies of choked flow through adiabatic and diabatic capillary tubes. Appl Therm Eng. 2015; 90:879-894.

[17] Pravin J, Neeraj A. A comparative study in the straight and a spiral adiabatic capillary tube. International journal of ambient energy. 2019; 40(7): 693-698.

[18] Ebrahim H, Saeed Z H, Mehdi S. Experimental investigation of pressure drop and heat transfer performance of amino acid-functionalized MWCNT in the circular tube. J Therm Anal Calorim. 2016; 124(1):205-214.

[19] Autee A T, Giri S V. Experimental study on two-phase flow pressure drop in small diameter bends. Perspectives in Science. 2016; 8: 621-625.

[20] Andrzejczyk R, Muszynski T, Dorao C A. Experimental investigations on adiabatic frictional pressure drops of R134a during flow in 5 mm diameter channel. Exp Therm Fluid Sci. 2017; 83: 78–87.

[21] Madanan U, Nayak R, Chatterjee D, Das S K. Experimental investigation on two-phase flow maldistribution in parallel minichannels with U-type configuration. The Canadian Journal of Chemical Engineering. 2018; 96: 1820-1828.

[22] Delishe C S, Welsford C A, Saghir M Z. Forced convection study with microporous channels and nanofluid: experimental and numerical. J Therm Anal Calorim. 2020; 140: 1205-1214.

[23] Banihashemi S, Assari M R, Javadi S, Vahidifar S. Experimental study of the effect of disk obstacle rotating with Different angular ratios on heat transfer and pressure drop in a pipe with turbulent flow. J Therm Anal Calorim. 2020; 1-16.

[24] Ajeel R K, Salim S I W. Experimental assessment of heat transfer and pressure drop of nanofluid as a coolant in corrugated channels. J Therm Anal Calorim. 2020; 1-13.

[25] Schmidt K A G, Maham Y, Mather A E. Use of the NRTL equation for simultaneous correlation of vapour-liquid equilibria and excess enthalpy. J Therm Anal Calorim. 2007; 89: 61-72.

[26] Lepori L, Gianni P, Matteoli E. Thermodynamic study of tetrachloromethane or heptane + cycloalkane mixtures. J Therm Anal Calorim. 2016; 124: 1497-1509.

[27] Matteoli E, Lepori L, Porcedda S. Thermodynamic study of mixtures containing dibromomethane. J Therm Anal Calorim. 2018; 132: 611-621.

[28] Peng D Y, Robinson D B. A new two-constant equation of state. Industrial and Engineering

Chemistry Fundamentals. 1976; 15(1): 92-94.

[29] Xia W, Li C, Jia W. An improved viscosity model based on Peng-Robinson equation of state for light hydrocarbon liquids and gases. Fluid Phase Equilib. 2014; 380: 147-151.

[30] Khosharay S. Suggestion of mixing rule for parameters of PRμ model for light liquid hydrocarbon mixtures. Korean J Chem Eng. 2014; 31(7): 1246-1252.

[31] Lin H, Duan Y Y. Empirical correction to the Peng-Robinson equation of state for the saturated region. Fluid Phase Equilib. 2005; 233(2): 194-203.

[32] Orbey H, Sandler S I. A comparison of various cubic equation of state mixing rules for the simultaneous description of excess enthalpies and vapor-liquid equilibria. Fluid Phase Equilib. 1996; 121(1): 67-83.

[33] Chen M, Xie Y, Wu H, Shi S, Yu J. Modeling solubility of nitrogen in clean fire extinguishing agent by Peng-Robinson equation of state and a correlation of Henry's law constants. Appl Therm Eng. 2016; 110: 457-468.

[34] McAdams W H, Woods W K, Heroman L C. Vaporization inside horizontal tubes: II. benzene-oil mixtures. Transactions of ASME. 1942; 64: 193-200.

[35] Cicchitti A, Lombaradi C, Silversti M. Two-phase cooling experiments: pressure drop, heat transfer and burnout measurements. Energia Nucleare. 1960; 7: 407-425.

[36] Dukler A E, Iii M W, Cleveland R G. Frictional pressure drop in two-phase flow: b. an approach through similarity analysis. AIChE J. 1964; 10(1): 44-51.

[37] Beattie D R H, Whalley P B. A simple two-phase frictional pressure drop calculation method. Int J Multiph Flow. 1982; 8(1): 83-87.

[38] Lin S, Kwok C C K, Li R Y, Chen Z H, Chen Z Y. Local frictional pressure drop during vaporization of R12 through capillary tubes. Int J Multiph Flow. 1991; 17(1): 95-102.

[39] Awad M M, Muzychka Y S. Effective property models for homogeneous two-phase flows. Exp Therm Fluid Sci. 2009; 33(1): 106-113.

[40] Ouyang L B, Aziz K. A homogeneous model for gas–liquid flow in horizontal wells. J Pet Sci Eng. 2000; 27: 119-128.

[41] Fang X, Xu Y, Zhou Z. New correlations of single-phase friction factor for turbulent pipe flow and evaluation of existing single-phase friction factor correlations. Nucl Eng Des. 2011; 241(3): 897-902.

[42] Li W, Wu Z. A general correlation for adiabatic two-phase pressure drop in micro/mini-channels. Int J Heat Mass Transf. 2010; 53(13): 2732-2739.

[43] Garcia J, Porto M P, Revellin R, Bonjour J, Machado L. An experimental study on two-phase frictional pressure drop for R-407C in smooth horizontal tubes. Int J Refrig. 2016; 73: 163-

174.

[44] Kim S M, Mudawar I. Universal approach to predicting two-phase frictional pressure drop for adiabatic and condensing mini/micro-channel flows. Int J Heat Mass Transf. 2012; 55(11): 3246-3261.

[45] Su J, Ruan S, Matlab 6.1 Practical Guide. Electronics Industry Press, Beijing. 2002.

[46] Wongwises S, Songnetichaovalit T, Lokathada N, Kritsadathikarn P K, Suchatawat M, Pirompak W. A comparison of the flow characteristics of refrigerants flowing through adiabatic capillary tubes. Int Commun Heat Mass Transf. 2000; 27(5): 611-621.

[47] Kim S M, Mudawar I. Universal approach to predicting two-phase frictional pressure drop for adiabatic and condensing mini/micro-channel flows. Int J Heat Mass Transf. 2012; 55: 3246–3261.

[48] Hossain M A, Afroz H M, Miyara A. Two-phase frictional multiplier correlation for the prediction of condensation pressure drop inside smooth horizontal tube, Procedia Eng. 2015; 105: 64–72.

[49] Jige D, Inoue N, Koyama S. Condensation of refrigerants in a multiport tube with rectangular minichannels. Int J Refr. 2016; 67: 202-213.

[50] Moradkhani M A, Hosseini S H, Valizadeh M, Zendehboudi A, Ahmadi G. A general correlation for the frictional pressure drop during condensation in mini/micro and macro channels. Int J Heat Mass Transf. 2020; 163: 120475.